Protein Structures

DOI: 10.1002/anie.201307955

Irreversible Denaturation of Proteins through Aluminum-Induced Formation of Backbone Ring Structures**

Bo Song, Qian Sun, Haikuo Li, Baosheng Ge, Ji Sheng Pan, Andrew Thye Shen Wee, Yong Zhang, Shaohua Huang, Ruhong Zhou, Xingyu Gao,* Fang Huang,* and Haiping Fang*

© 2014 Wiley-VCH Verlag GmbH & Co. KGaA, Weinheim

Abstract: *A combination of ab initio calculations, circular dichroism, nuclear magnetic resonance, and X-ray photoelectron spectroscopy has shown that aluminum ions can induce the formation of backbone ring structures in a wide range of peptides, including neurodegenerative disease related motifs. These ring structures greatly destabilize the protein and result in irreversible denaturation. This behavior benefits from the ability of aluminum ions to form chemical bonds simultaneously with the amide nitrogen and carbonyl oxygen atoms on the peptide backbone.*

Aluminum is widely used in antimicrobial coagulants,[1–5] food additives, and cookware.[6] However, it has been reported that high doses of aluminum can cause neurotoxicity,[7] which is associated with an altered function of the blood–brain barrier.[8] There are many examples of aluminum neurotoxicity in animals and in humans, with evidence linking clinical disorders to aluminum exposure.[9–19] Such illnesses include Parkinson's disease,[9] Alzheimer's disease,[10–14] amyotrophic lateral sclerosis,[15] macrophagic myofasciitis,[16] anemia,[17] bone marrow fibrosis,[17] renal dysfunction, and chronic renal failure.[18] It has been hypothesized that Al is a critical factor in the etiopathogenesis of neurodegenerative diseases, particularly Alzheimer's disease.[10–12] Despite this close relationship between aluminum and health, the mechanisms behind these aluminum-related diseases are poorly understood, especially on the molecular level, which limits efforts to prevent and treat these diseases.

By using a combined approach with ab initio calculations, circular dichroism (CD), nuclear magnetic resonance (NMR), and X-ray photoelectron spectroscopy (XPS) we show herein that aluminum ions can surprisingly induce the formation of backbone ring structures in a wide range of peptides, including neurodegenerative disease related motifs. These ring structures largely destabilize the protein and result in irreversible denaturation. This behavior benefits from the ability of aluminum ions to form chemical bonds simultaneously with both the amide nitrogen and carbonyl oxygen atoms on the peptide backbone.[20] The XPS experiments, in particular, strongly support the theoretical prediction that the aluminum ions bound to the protein are reduced to a large extent from Al^{3+} ions through the simultaneous bonds to the nitrogen and oxygen atoms. These findings provide a molecular-level understanding of the potential mechanism underlying aluminum-induced neurotoxicity, and may be helpful in novel drug design for aluminum-related diseases, and even provide clues for the treatment of aluminum-polluted water.

To illustrate the formation of an Al-induced backbone ring structure in a peptide, we first modeled theoretically the interactions of the poly-Ala peptide HCO-$[Ala]_n$-NH_2 (Figure 1 a,d) and the hydrated Al ion $[AlOH(H_2O)_4]^{2+}$ (Figure 1 a). HCO-$[Ala]_n$-NH_2 represents a typical motif in a neurodegenerative-disease-related protein.[21] The five-

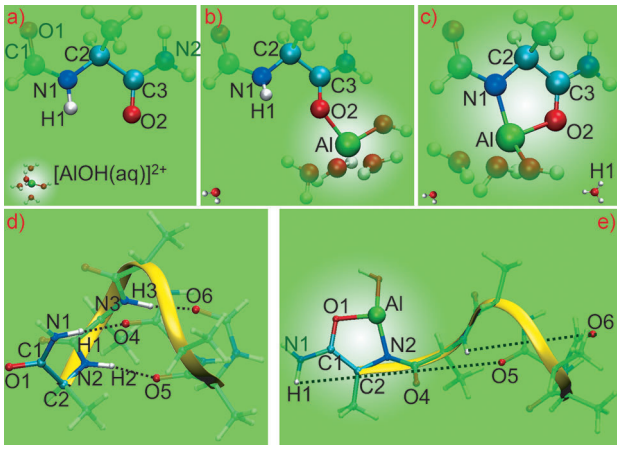

Figure 1. A hydrated Al ion binds to a peptide backbone and forms a ring structure, thereby resulting in damage to the peptide helix. The cyan, blue, red, white, and green balls represent C, N, O, H, and Al, respectively. The yellow ribbon represents the peptide backbone. The black dotted lines indicate hydrogen bonds. a) The initial state: a peptide HCO-Ala-NH_2 and a hydrated Al ion $[AlOH(H_2O)_4]^{2+}$ separated by a wide distance. b) State I: binding of the Al ion with the O2 atom in the peptide backbone. c) State II: simultaneous binding of the Al ion with the atoms N1 and O2 of the backbone, thereby inducing formation of a ring structure. d,e) A long peptide HCO-$[Ala]_5$-NH_2: a helix with three hydrogen bonds (d); severe damage of the helix and the hydrogen bonds caused by the Al-induced ring (e); the water molecules are not presented for clarity.

[*] Prof. Dr. B. Song, Dr. H. Li, X. Gao, H. Fang
Shanghai Institute of Applied Physics, Chinese Academy of Sciences
P. O. Box 800-204, Shanghai 201800 (China)
E-mail: bosong@sinap.ac.cn
xingyugao@sinap.ac.cn
Dipl. Q. Sun, Dr. B. Ge, Prof. Dr. F. Huang
Center for Bioengineering and Biotechnology
China University of Petroleum (Huadong)
Changjiang West Road 66, Qingdao 266580 (China)
E-mail: fhuang@upc.edu.cn
Dr. J. S. Pan
Institute of Materials Research and Engineering
Singapore 117602 (Republic of Singapore)
Prof. Dr. A. T. S. Wee
Physics Department, National University of Singapore
Singapore 117542 (Republic of Singapore)
Dr. Y. Zhang
College of Chemistry and Molecular Engineering, Peking University
Beijing 100871 (China)
Dr. S. Huang
Qingdao Institute of Bioenergy and Bioprocess Technology
Chinese Academy of Sciences
Qingdao 266101 (China)
Dr. R. Zhou
IBM Thomas J. Watson Research Center
New York, NY 10598 (USA)

[**] We thank Prof. Dr. W. Liu, H. Jiang, Y. Gao, and J. Gao for helpful discussions. This work was supported by the NSFC (11174310, 11290164, 21073236), NBRPC (2010CB934504), KIPCAS, NSFDYSSP (JQ201008), PNCETUMEC (NCET-10-0815), the Shanghai Supercomputer Center of China, and the Supercomputing Center of the Chinese Academy of Sciences.

Supporting information for this article is available on the WWW under http://dx.doi.org/10.1002/anie.201307955.

 © 2014 Wiley-VCH Verlag GmbH & Co. KGaA, Weinheim

coordinate hydrated Al ion can exist in the biochemically critical pH range of 4.3 to 7.0.[22]

First, the hydrated Al ion can strongly interact with an oxygen atom on the peptide backbone. The resulting state is referred to as State I (Figure 1b), in which the hydrated Al ion bound to the oxygen atom O2 (-O2-) on the backbone is denoted as -O2-AlOH(aq), with "aq" denoting the water molecules in the hydration sphere. The binding energy of this state was computed by an ab initio method based on the second-order Møller–Plesset perturbation theory (MP2).[23] The binding energy (Figure 2) reaches $-27.05\ \text{kcal mol}^{-1}$ ($-45.36\ k_B T$ at $T = 300$ K), which means that the hydrated

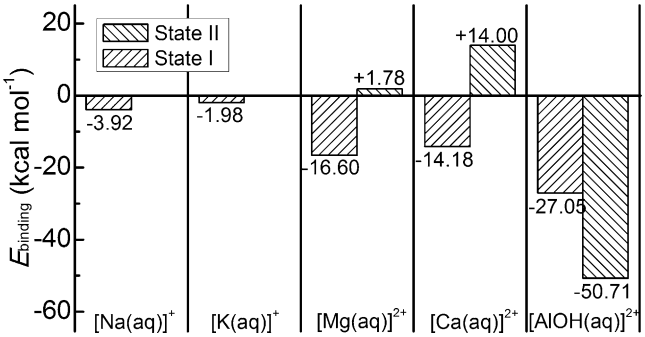

Figure 2. Binding energies ($E_{binding}$) of the hydrated ions $[AlOH(aq)]^{2+}$ and $[M(aq)]^{n+}$ in State I and State II. "aq" denotes the water molecules in the hydration sphere. $n = 1$ for "M" = Na or K, $n = 2$ for "M" = Mg or Ca.

Al ion is stably bound to -O2-, while one water molecule initially bound to the Al ion is released. Our classical molecular dynamics (MD) simulations indicate that the Al ion can easily diffuse to be near the oxygen atom of the backbone (see the detailed MD results in Section 2.1 of the Supporting Information). Therefore, -O2- can stably bond to the Al ion in water.

The Al ion in -O2-AlOH(aq) can further interact with the nitrogen atom N1 (-N1-) neighboring -O2- on the peptide backbone, thereby resulting in a ring structure that includes Al, N1, and O2, as well as the two neighboring carbon atoms C2 and C3 in the backbone (Figure 1c). This state is referred to as State II (denoted -O2-Al[OH(aq)]-N1-). The binding energy of State II (Figure 2) reaches $-50.71\ \text{kcal mol}^{-1}$ ($-85.04\ k_B T$ at $T = 300$ K), which indicates that the Al ion bound to the backbone is more stable in State II than in State I. The hydrogen atom H1 initially bound to -N1- is substituted by the Al ion, while one water molecule initially bound to the Al ion is released. Occupied valence orbitals of the structure -O2-Al[OH(aq)]-N1- contain electrons from the Al ion as well as the -N1- and -O2- atoms. For example, Al and -N1- are connected through the highest occupied molecular orbital (HOMO; Figure 3a), while Al, -N1-, and -O2- are connected through the occupied orbital HOMO-5 (Figure 3b). Moreover, natural-bond-orbital (NBO) analysis[24] indicates that an Al–N1 bond is composed of 9.4% from the Al valance orbitals and 90.6% from the -N1- valance orbitals, while an Al–O2 bond is composed of 7.3% from the Al valance orbitals and 92.7% from the -O2- valance orbitals.

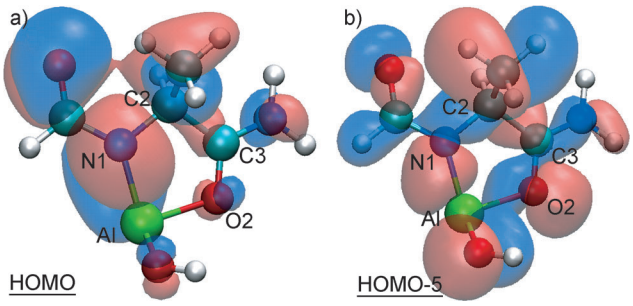

Figure 3. HOMO (a) and HOMO-5 (b) orbitals, as examples of the occupied valence orbitals involving Al in State II. The cyan, blue, red, white, green balls represent C, N, O, H, and Al, respectively. The surface denotes the orbital. The water molecules are not shown for clarity.

Furthermore, we found that the Al ion bound with the peptide in State II only had a Mulliken charge[25] of $+0.94\,e$, which indicates that the Al ion in the peptide is largely reduced compared to a Al^{3+} ion. Therefore, the Al-induced ring formation in the presence of water is largely due to both the ionic and covalent nature of the bonds between the Al ion and the nitrogen or oxygen atoms on the peptide backbone.

Numerical simulations using an ab initio method based on density functional theory (DFT) suggest that the Al-induced ring can destroy the peptide helix irreversibly under biochemical conditions. Without the Al ion (Figure 1d,f), this peptide forms a helix that is stabilized by three hydrogen bonds N1–H1···O4, N2–H2···O5, and N3–H3···O6, with a hydrogen–oxygen distance of about 1.80 Å. When an Al ion induces ring formation (Figure 1e,g), the H1···O4 and H3···O6 distances become much larger, and the N2–H2 bond in N2–H2···O5 is cleaved. These changes indicate severe damage to the helix. More interestingly, the dihedral angle O1-C1-C2-N2 in the original helix can rotate freely; however, it is now rigidly fixed at around 179° through the formation of the Al-induced ring with a strong binding energy of $-50.71\ \text{kcal mol}^{-1}$ ($-85.04\ k_B T$ at $T = 300$ K). Thus, the damage to the helix is irreversible under biochemical conditions. We expect that the Al-induced rings will also lead to misfolded structures in β-sheets, similar to α-helices, as a consequence of their severe influence on the peptide backbone. These misfolded structural units in the protein backbone will undoubtly lead to serious damage to the secondary structures.

We have further investigated the behaviors of other ions (Na^+, K^+, Mg^{2+}, and Ca^{2+}) to show that the Al ion is uniquely involved in the formation of the ring structure. We computed the binding energies of other hydrated ions $[M(H_2O)_6]^{n+}$ ($n =$ 1 for M = Na or K, $n = 2$ for M = Mg or Ca) bound to the backbone in the same manner as the hydrated Al ion in States I and II. The binding energies in State I (Figure 2) for the hydrated Na ($-3.92\ \text{kcal mol}^{-1}$) and K ($-1.98\ \text{kcal mol}^{-1}$) ions is comparable to the thermal fluctuation in water at room temperature, which means that Na^+ and K^+ cannot be stably bound to -O2-. The binding energies for Mg^{2+} and Ca^{2+} ions in State I are more than $10\ \text{kcal mol}^{-1}$ less than that of the Al ion, which indicates that a potential Mg- or Ca-induced

© 2014 Wiley-VCH Verlag GmbH & Co. KGaA, Weinheim

State I would be substantially less stable than State I for the Al ion. Moreover, the positive binding energies of the Mg- and Ca-induced State II indicates that these states are unstable. Thus, unlike the Al ion, Mg^{2+}, Ca^{2+}, Na^{+}, and K^{+} ions cannot induce ring formation on the backbone, since the bonds involving these ions do not have as much covalent character as the involved Al bonds.

To validate these surprising findings of the Al ion induced peptide conformational changes, we performed circular dichroism (CD) experiments with the N-terminal domain of phosphoglycerate kinase (PGK, Protein Data Bank (PDB) code 1PHP, see Section 2.2 in the Supporting Information for details) as an example, which is related to mental disorders.[26] As reported in the literature[27] and demonstrated herein, this PGK domain can thermally unfold and refold reversibly (on adjustment of the temperature), and is rich in nonpolar and neutral amino acids (e.g. glycine, alanine, and valine; see Figure S2 in the Supporting Information).

CD data (Figure 4) suggest that only Al ions have a strong influence on the PGK denaturation process and can induce irreversible denaturation. The CD signals reach the first plateau when the temperature reaches about 338 K, and then suddenly increase at about 353 K to the second plateau. Further experiments show that the CD signals can recover if

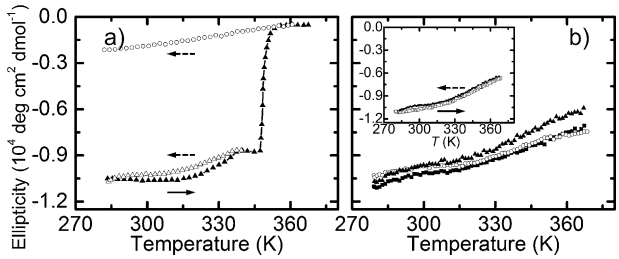

Figure 4. Thermodenaturation of PGK protein monitored by CD spectroscopy. a) PGK in the presence of $Al_2(SO_4)_3$. ▲, △, and ○ curves denote the CD signals as the temperature increases from 278 to 368 K, decreases from the first plateau to 278 K, and decreases from the second plateau to 278 K, respectively. b) PGK in the presence of K_2SO_4 (○), $MgSO_4$ (■), and $CaSO_4$ (▲) as the temperature increases from 278 to 368 K. No irreversible denaturation is observed. Inset: the signals in the presence of $MgSO_4$, as an example of denaturation (■) and recovery (□).

the temperature is decreased once the first plateau is reached, but cannot recover from the second plateau. These findings indicate that the first denaturation is reversible, but the second one is irreversible. Moreover, aggregates were clearly observed in the irreversibly denatured state. In contrast, the addition of K^{+}, Mg^{2+}, or Ca^{2+} ions does not change the PGK stability (Figure 4b). These observations unambiguously suggest that the altered denaturation behaviors of the protein are due to the Al ions, which is consistent with the theoretical results.

The change in the PGK denaturation in the presence of Al ions can be attributed to the strong interaction between PGK and Al ions. As predicted theoretically, the Al ion can form a very stable State II with unfolded peptide, potentially changing the equilibrium between the native and denatured states. Meanwhile, as suggested by the CD and NMR experiments (see Section 2.4 of the Supporting Information for details), the Al-bound denatured state can irreversibly form aggregates, further shifting the equilibrium.

We performed X-ray photoelectron experiments with the irreversibly denatured and aggregated PGK protein to demonstrate that the Al ion is simultaneously bound to the amide nitrogen and carbonyl oxygen atoms of the peptide backbone. There are two peaks in the X-ray photoelectron spectrum at 117.3 ± 0.2 eV and 122.6 ± 0.2 eV (Figure 5a).

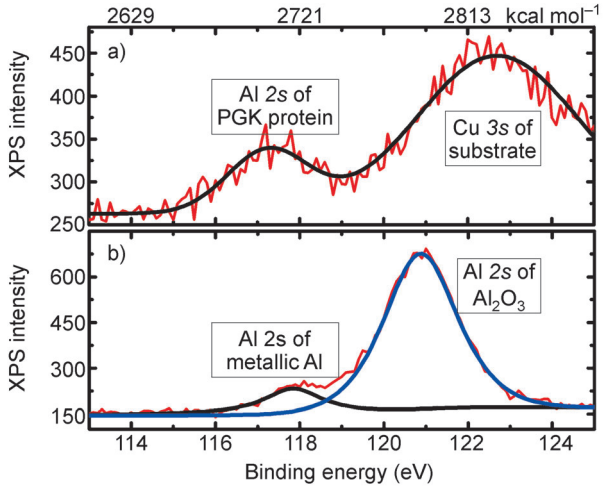

Figure 5. X-ray photoelectron spectra (red curve) together with the fitting curves. a) The irreversibly denatured and aggregated PGK protein on the copper substrate. The peak (fitted by a black curve) at 117.3 ± 0.2 eV falls in the area of elemental Al 2s. The peak (fitted by a black curve) at 122.6 ± 0.2 eV comes from the copper substrate (Cu 3s). b) The oxidized Al metal. The peak (fitted by a black curve) at 117.8 ± 0.2 eV comes from metallic Al, while the peak (fitted by a blue curve) at 120.8 ± 0.2 eV comes from Al_2O_3.

For comparison, we have also measured the spectra of metallic Al and Al_2O_3 (Figure 5b), which have peaks at 117.8 ± 0.2 eV and 120.8 ± 0.2 eV, respectively. The spectra of the metallic Al and Al_2O_3 are consistent with the reported values of 117.7 eV for metallic Al[28] and the value of 121.0 eV for an Al^{3+} ion in Al_2O_3,[29] respectively. Interestingly, although the Al in the aggregated PGK protein has clear bonds with neighboring atoms, the peak at 117.3 ± 0.2 eV in the spectrum of the aggregated PGK protein is very close to the value of 117.8 ± 0.2 eV in the spectrum of the Al 2s level of metallic Al, and considerably smaller than the value of 120.8 ± 0.2 eV in the spectrum of the Al^{3+} ions from Al_2O_3. Therefore, the Al ions in the aggregated PGK protein are very similar to metallic Al, and much different from Al^{3+} ions. This agrees well with the theoretical prediction that the Al ions bound to the peptide are reduced to a large extent from Al^{3+} ions. It should be noted that the peak centered at 122.6 ± 0.2 eV is in the area of a Cu 3s photoemission,[30] which indicates that it comes from the Cu substrate.

We have calculated the binding energy of the 2s electron of the Al ion bound simultaneously with the amide nitrogen and carbonyl oxygen atoms of the peptide (-O2-Al[OH(aq)]-

 © 2014 Wiley-VCH Verlag GmbH & Co. KGaA, Weinheim

N1-) through an ab initio method based on relativistic density functional theory (RDFT).[31] As a comparison, the binding energies of the 2s electron of the Al^{3+} ions in AlF_3 and $AlCl_3$ were also calculated. Here we used AlF_3 and $AlCl_3$ (to provide a range), instead of Al_2O_3, because it is still nontrivial to directly calculate the XPS spectra, since the current approaches for metallic Al and Al_2O_3 are still under development. On the other hand, the electronegativity of O at 3.610 falls in-between that of F (4.193) and Cl (2.869),[32] thus it might be reasonable to use AlF_3 and $AlCl_3$ to estimate a range for Al_2O_3. Table 1 summarizes the detailed comparisons for

Table 1: Comparison of binding energies of the Al 2s electron by RDFT calculations $\left(E_{binding}^{RDFT}\right)$ and XPS experiments ($E_{binding}^{XPS}$, peaks in XP spectra), as well as the binding energies of the Al ion bound to the peptide relative to that of a Al^{3+} ion.[a]

	Al ion in peptide	Trivalent Al ion	Relative binding energy
$E_{binding}^{RDFT}$ [eV]	118.7	122.1[b]	−3.4
		121.3[c]	−2.6
$E_{binding}^{XPS}$ [eV]	117.3 ± 0.2	120.8 ± 0.2[d]	−3.5 ± 0.4

[a] As a result of the different energy shifts in XPS instruments and in RDFT calculations, there are some discrepancies in the absolute binding energies; however, the relative binding energies agree very well between the theory and experiment, which we believe is of more importance, since it captures the "environmental difference" of the Al ions in the peptide and of an Al^{3+} ion. The good agreement of the relative binding energies between the RDFT calculations and XPS experiments strongly supports our theoretical prediction that the Al ion in the peptide has the structure -O2-Al[OH(aq)]-N1-. [b] Calculated data of Al^{3+} in AlF_3. [c] Calculated data of Al^{3+} in $AlCl_3$. [d] Experimental result of Al^{3+} in Al_2O_3.

the relative binding energies of the Al ion in protein environments and the Al^{3+} ion from both DFT theory and XPS experiments. Our DFT calculations show an average relative binding energy of −3.0 eV (using both AlF_3 and $AlCl_3$ as a base), which agrees very well with that of -3.5 ± 0.4 eV from our XPS experiment (using Al_2O_3 as a base), which indicates that the Al ions bound to proteins are reduced. Therefore, the XPS observations of the irreversibly denatured and aggregated PGK protein strongly support the theoretical prediction that the Al ion forms chemical bonds simultaneously with the N and O atoms in the form of -O2-Al[OH(aq)]-N1- in the aggregated PGK protein.

As a control XPS experiment, we used a PGK sample prepared with both Al and Mg ions in the solution. This sample exhibits only Al photoemission features (see Figure S3b in the Supporting Information) without any traces related to Mg species within the sensitivity of the experiment. These findings indicate that the Mg ion, unlike the Al ion, cannot interact strongly with the protein.

In summary, based on both theoretical analysis and experiments, we show that Al ions can unexpectedly induce ring structures in the backbone of a protein, largely destroying the secondary structures of the protein. This particular behavior of the Al ion lies in its ability to form chemical bonds (with both covalent and ionic characteristics) with the amide nitrogen and carbonyl oxygen atoms on the backbone. These findings provide a novel mechanism for Al ions interacting with biomolecules, which may have significance in the fields of medicine, biotechnology, and environmental science.

Materials and Methods

Computations using ab initio methods: The calculations on the short peptide HCO-Ala-NH_2 ($C_4N_2O_2H_8$) were performed using an ab initio method based on second-order Møller–Plesset perturbation theory (MP2). To realize the relaxation of the long peptide HCO-$[Ala]_5$-NH_2, we applied an ab initio method based on density functional theory (DFT). The calculations above were carried out using the Gaussian-09 package. Considering the relativistic effect of core electrons, the binding energy of the 2s electron of the Al ion simultaneously bound to the amide nitrogen and carbonyl oxygen atoms in the peptide (-O2-Al[OH(aq)]-N1-) was calculated by the ab initio method based on relativistic density functional theory (RDFT) with the BDF package.[31]

Classical molecular dynamics simulations: We performed classical dynamics simulations using poly-Ala peptide $[Ala]_5$ in $AlCl_3$ solution with Gromacs 4.0. Considering that an Al ion in water usually binds to one hydroxy group under the biochemically critical pH range of 4.3 to 7.0, we applied a form of $[Al\text{-}OH]^{2+}$.

Circular dichroism spectra: Denaturation experiments were performed using several salts, including $Al_2(SO_4)_3$, K_2SO_4, $MgSO_4$, and $CaSO_4$. The N-terminal domain of PGK was dissolved in sodium acetate buffer. The experiments were carried out at temperatures between 278 and 368 K.

X-ray photoelectron spectra: Two samples were prepared for X-ray photoelectron experiments: 1) the PGK protein mixed with $Al_2(SO_4)_3$; 2) the PGK protein with both $Al_2(SO_4)_3$ and $MgSO_4$. The XPS experiments were performed using a VG ESCALAB 220i-XL instrument equipped with a monochromatic Al Ka source (1486.7 eV photons), a concentric hemispherical analyzer, and a magnetic immersion lens (XL lens) to increase the sensitivity of the instrument. The instrument was calibrated with pure gold. All spectra were recorded in the constant pass energy mode of the analyzer using the monochromatic Al Ka X-ray source.

Full Methods and any associated references are available in Section 1 of the Supporting Information.

Received: September 10, 2013
Revised: March 24, 2014
Published online: April 28, 2014

Keywords: aluminum · aluminum-related diseases · peptides · protein denaturation

[1] S. R. Farrah, S. M. Goyal, C. P. Gerba, C. Wallis, J. L. Melnick, *Appl. Environ. Microbiol.* **1978**, *35*, 624–626.
[2] R. G. Gilbert, C. P. Gerba, R. C. Rice, H. Bouwer, C. Wallis, J. L. Melnick, *Appl. Environ. Microbiol.* **1976**, *32*, 333–338.
[3] J. C. Lance, C. P. Gerba, *Appl. Environ. Microbiol.* **1984**, *47*, 484–488.
[4] T. P. Monath, E. Fowler, C. T. Johnson, J. Balser, M. J. Morin, M. Sisti, D. W. Trent, *N. Engl. J. Med.* **2011**, *364*, 1326–1333.
[5] K. J. Ishii, F. Bureau, C. J. Desmet, *Nat. Med.* **2011**, *17*, 996–1002.
[6] The right to water: World Health Organization (WHO), Geneva, Switzerland, **2003**.
[7] D. Krewski, et al., *J. Toxicol. Environ. Health B Crit. Rev.* **2007**, *10*, 1–269.
[8] W. A. Banks, A. J. Kastin, *Neurosci. Biobehav. Rev.* **1989**, *13*, 47–53.
[9] S. Bolognin, L. Messori, P. Zatta, *Neuromol. Med.* **2009**, *11*, 223–238.

 © 2014 Wiley-VCH Verlag GmbH & Co. KGaA, Weinheim

[10] G. Farrar, J. A. Blair, P. Altmann, S. Welch, O. Wychrij, B. Ghose, J. Lejeune, J. Corbett, V. Prasher, *Lancet* **1990**, *335*, 747 – 750.
[11] C. R. Harrington, C. M. Wischik, F. K. McArthur, G. A. Taylor, J. A. Edwardson, J. M. Candy, *Lancet* **1994**, *343*, 993 – 997.
[12] L. Tomljenovic, *J. Alzheimer's Dis.* **2011**, *23*, 567 – 598.
[13] I. Shcherbatykh, D. O. Carpenter, *J. Alzheimer's Dis.* **2007**, *11*, 191 – 205.
[14] V. Rondeau, D. Commenges, H. Jacqmin-Gadda, J. F. Dartigues, *Am. J. Epidemiol.* **2000**, *152*, 59 – 66.
[15] F. P. Thinnes, *Mol. Genet. Metab.* **2010**, *101*, 299 – 300.
[16] E. Israeli, N. Agmon-Levin, M. Blank, Y. Shoenfeld, *Clin. Rev. Allergy Immunol.* **2011**, *41*, 163 – 168.
[17] M. R. Wills, J. Savory, *Lancet* **1983**, *322*, 29 – 34.
[18] I. B. Salusky, J. Foley, P. Nelson, W. G. Goodman, *N. Engl. J. Med.* **1991**, *324*, 527 – 531.
[19] C. Exley, E. R. House in *Aluminium in the human brain. Metal Ions in Neurological Systems* (Eds.: W. Linert, H. Kozlowski), Springer, Heidelberg, **2012**, pp. 95 – 102.
[20] a) T. Holtrichter-Rößmann, J. Isermann, C. Rösener, B. Cramer, C.-G. Daniliuc, J. Kösters, M. Letzel, E.-U. Würthwein, W. Uhl, *Angew. Chem.* **2013**, *125*, 7275 – 7278; *Angew. Chem. Int. Ed.* **2013**, *52*, 7135 – 7138; b) F. A. Cotton, G. Wilkinson, *Advanced inorganic chemistry: A comprehensive text*, Interscience Publishers, Wiley, New York, **1962**.
[21] a) H.-D. Du, L. Tang, X.-Y. Luo, H.-T. Li, J. Hu, J.-W. Zhou, H.-Y. Hu, *Biochemistry* **2003**, *42*, 8870 – 8878; b) S. Zhang, A. Rich, *Proc. Natl. Acad. Sci. USA* **1997**, *94*, 23 – 28; c) A. Grupi, E. Hass, *J. Mol. Biol.* **2011**, *405*, 1267 – 1283; T. Wolter, T. Steinbrecher, M. Elstner, *PLoS ONE* **2013**, *8*, e58774.
[22] T. W. Swaddle, J. Rosenqvist, P. Yu, E. Bylaska, B. L. Phillips, W. H. Casey, *Science* **2005**, *308*, 1450 – 1453.
[23] a) C. Møller, M. S. Plesset, *Phys. Rev.* **1934**, *46*, 618 – 622; b) M. Duan, B. Song, G. Shi, H. Li, G. Ji, J. Hu, X. Chen, H. Fang, *J. Am. Chem. Soc.* **2012**, *134*, 12104 – 12109.
[24] A. E. Reed, L. A. Curtiss, F. Weinhold, *Chem. Rev.* **1988**, *88*, 899 – 926.
[25] R. S. Mulliken, *I. J. Chem. Phys.* **1955**, *23*, 1833 – 1840.
[26] a) L. R. Chiarelli, S. M. Morera, P. Bianchi, E. Fermo, A. Zanella, A. Galizzi, G. Valentini, *PLoS ONE* **2012**, *7*, e32065; b) J. Song, *J. Biol. Chem.* **2003**, *278*, 24714 – 24720.
[27] N. Ballery, P. Minard, M. Desmadril, J.-M. Betton, D. Perahia, L. Mouawad, L. Hall, J. M. Yon, *Protein Eng.* **1990**, *3*, 199 – 204.
[28] M. Oku, N. Masahashi, S. Hanada, K. Wagatsuma, *J. Alloys Compd.* **2006**, *413*, 239 – 243.
[29] N. R. Rajopadhye, S. B. Dake, S. V. Bhoraskar, *Thin Solid Films* **1986**, *142*, 127 – 138.
[30] A. N. Mansour, *Surf. Sci. Spectra* **1994**, *3*, 202 – 210.
[31] a) W. Liu, G. Hong, D. Dai, L. Li, M. Dolg, *Theor. Chem. Acc.* **1997**, *96*, 75 – 83; b) W. Liu, F. Wang, L. Li, *J. Theor. Comput. Chem.* **2003**, *2*, 257 – 272.
[32] L. C. Allen, *J. Am. Chem. Soc.* **1989**, *111*, 9003 – 9014.

 © 2014 Wiley-VCH Verlag GmbH & Co. KGaA, Weinheim